

A comprehensive deposition velocity model for slurry transport in horizontal pipelines

Ben Bbosa¹ · Emmanuel DelleCase¹ · Michael Volk¹ · Evren Ozbayoglu¹

Received: 28 September 2015 / Accepted: 22 May 2016 / Published online: 8 June 2016
© The Author(s) 2016. This article is published with open access at Springerlink.com

Abstract Transportation of solids in form of slurries has become one of the most important unit operations in industries across several disciplines. In fact, the need is more pronounced in industries that are very important for human survival such as food processing, pharmaceuticals and energy (coal, oil and gas). A lot of work has been done in the past 30 years in understanding the factors affecting the deposition velocity of solids in slurries. Experimental observation and theoretical predictions pointed to mixture velocity and solid/fluid properties especially rheology of the resulting slurry to be the most important factors that dramatically affect particle motion and patterning. This paper presents a critical deposition velocity model and a “stability flow map” for complex rheology slurries. The critical deposition model utilizes a more robust generalized two-parameter rheology model to account for any given slurry rheology. The “stability flow map” demarcates the different flow patterns that may be observed at different mixture velocities and rheologies. On this map, the homogeneous slurries are predicted at low rheology and high mixture velocity, whereas heterogeneous slurries (with a concentration gradient) predicted at high rheology (yield stress effects). Sensitivity analysis was conducted on critical Reynolds number, particle density, carrier fluid density, generalized flow behavior index and pipe diameter. It was observed that increase in shear thinning behavior, particle density, pipe diameter and particle diameter led to a decrease in the laminar region and an increased unstable region. The model showed good

performance when tested on glass and stainless steel beads test data available in open literature. Preliminary simulation with this map may help engineers select flowline size and carrier fluid rheology for a given type of solid particle.

Keywords Rheology · Particulate flow · Slurry · Flow regime · Flow assurance · Stability map

List of symbols

$1-C_s$	Liquid volume fraction (–)
C_s	Solid particle volume fraction (–)
D	Pipe inner diameter (m)
d	Particle diameter (micron)
g	Gravity (ms^{-2})
K	Viscosity consistency coefficient (mPa s^N)
n	Flow behavior index/power law exponent (–)
N	Generalized flow behavior index (–)
Re_G	Generalized Reynolds number (–)
$Re_{G,t}$	Generalized transitional Reynolds number (–)
S	Ratio of solid density to carrier fluid density, ρ_s/ρ_f (–)
V	Velocity (ms^{-1})
V_c	Critical deposition velocity (ms^{-1})
V_l	Laminar deposition velocity (ms^{-1})
V_t	Transitional deposition velocity (ms^{-1})
x_c	Ratio of yield stress to wall shear stress, τ_y/τ_w (–)
α	Ratio of wall shear stress to surficial particle shear stress, τ_w/τ_p (–)
η_m	Viscosity function (mPa s^N)
μ	Viscosity (mPa s)
μ_B	Plastic viscosity (mPa s)
μ_m	Mixture fluid viscosity (mPa s)
μ_w	Carrier fluid viscosity (mPa s)
ρ	Density (kg m^{-3})

✉ Ben Bbosa
emmanuel-bbosa@utulsa.edu

¹ SPE, The University of Tulsa, Tulsa, OK, USA

ρ_f	Carrier fluid density (kg m^{-3})
ρ_s	Solid density (kg m^{-3})
τ	Shear stress (Pa)
τ_w	Wall shear stress (Pa)
τ_p	Surficial particle shear stress (Pa)
τ_y	Yield stress (Pa)
χ	Hindered settling factor (–)
\mathbb{K}	Generalized viscosity consistence coefficient (mPa s^N)

Introduction

One of the main concerns in solid transport is pipeline plugging. Plugging is not only a safety threat but also a financial one. Plugging can lead to frequent shutdowns, equipment damage and even explosions. Deposition velocity determination is one of the design philosophies that can be employed to evaluate plugging potential. Deposition velocity is the velocity below which particles begin to deposit forming moving or stationary beds at the bottom of the pipe (Poloski et al. 2009a, b; Yokuda et al. 2009; Turian et al. 1987; Peysson 2004; Doron and Barnea 1996; Ibarra et al. 2014). This causes the flow to become unstable, and the pipe will eventually clog. Partial pipeline blockages may lead to erosion, corrosion and local velocity increase (Najmi et al. 2015). Plugging results from transporting slurries at velocities lower than the deposition velocity (Ibarra et al. 2014; Najmi et al. 2015; Salama 2000; King et al. 2001; McLaury et al. 2011; Al-lababidi et al. 2012). Most deposition models and experimental investigation in open literature focus on Newtonian carrier fluids. The goal of this work is to extend deposition velocity modeling to non-Newtonian fluids. Since deposition velocity is associated with flow regime changes, a flow regime map will be developed in this work. Finally, a predictive method is developed for the deposition velocity and flow regimes.

Solid transport phenomena: flow regimes and the stability map

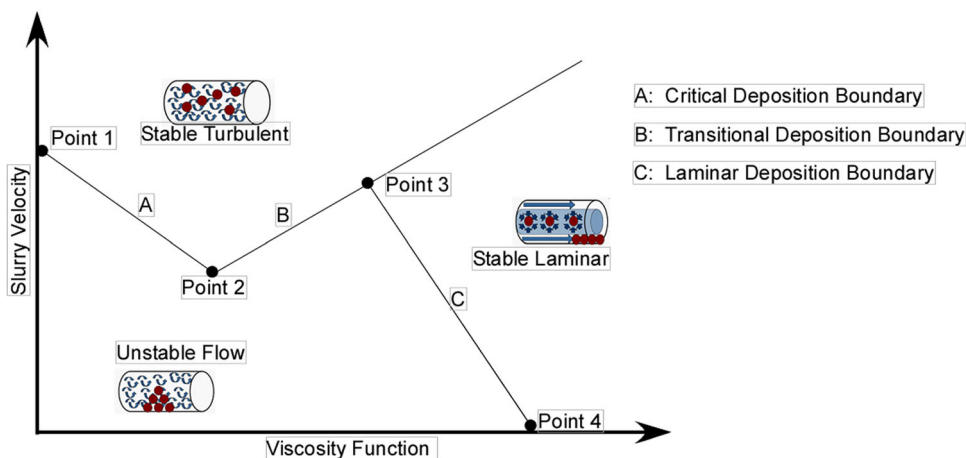
Transportability of solids in pipelines strongly depends on particle distribution (Poloski et al. 2009a; Ibarra et al. 2014). Solid particle distribution in pipelines is dictated by carrier fluid properties, solid properties, flow geometry and flow conditions such as velocity (Poloski et al. 2009a, b; Yokuda et al. 2009; Turian et al. 1987; Ibarra et al. 2014; Najmi et al. 2015; Salama 2000; King et al. 2001; McLaury et al. 2011; Al-lababidi et al. 2012; Ozbayoglu 2002; Gillies et al. 2007; Rensing et al. 2008; and Ma and Zhang

2008). Several flow regimes have been proposed by different researchers including Durand (1953), Newitt et al. (1955), Turian et al. (1987), Turian and Yuan (1977), Doron and Barnea (1996), Peysson (2004) and most recently (Ramsdell and Miedema 2013).

In the present study, three main solid flow regimes are considered including unstable regime, stable turbulent regime and stable laminar regime.

- *Stable turbulent regime* At sufficiently high flow velocities, the eddy forces are sufficient to suspend the particles in the liquid phase and maintain a uniform dispersion (Poloski et al. 2009a, b; Yokuda et al. 2009; Turian et al. 1987; Peysson 2004; Doron and Barnea 1996). The velocity required to reach turbulent flow depends on fluid rheological properties (Poloski et al. 2009a, b; Yokuda et al. 2009). Since particles are dispersed uniformly in the liquid phase, this regime is sometimes referred to as pseudo-homogeneous phase or simply slurry (Peysson 2004; Doron and Barnea 1996). It is characterized by a symmetrical solid distribution in the radial direction (Peysson 2004; Doron and Barnea 1996). It is the most desired regime for solid transport; however, it is achieved at high velocities (Doron and Barnea 1996) and it is associated with erosion due to radial particle movement (Peysson 2004; Salama 2000).
- *Stable laminar regime* At high yield stresses, yield stress forces become dominant and sufficient to suspend the particles in the core (Poloski et al. 2009a, b). Also, particles close to the pipe wall are pushed by the wall shear stress. This regime is characterized by the presence of solid particle concentration gradient perpendicular to the flow direction (Poloski et al. 2009a, b; Yokuda et al. 2009; Turian et al. 1987; Peysson 2004; Doron and Barnea 1996; Ibarra et al. 2014; Najmi et al. 2015; Salama 2000; King et al. 2001). Because of this non-uniform particle distribution, this regime is sometimes referred to as heterogeneous flow regime (Peysson 2004; Doron and Barnea 1996; Ibarra et al. 2014; Najmi et al. 2015). This is the most practical solid transport regime for high viscosity and/or high yield stress fluids.
- *Unstable regime* Consider fluids with low or no yield stress at flowing velocities, the eddy forces and/or yield stress forces are not sufficient to suspend the solid particles. Therefore, particles move to pipe bottom (Poloski et al. 2009a, b). This regime is characterized by a stationary bed at the bottom of the pipe and solid transportation is achieved through saltation (Peysson 2004; Doron and Barnea 1996). This regime is referred to as unstable because solid concentration is not constant with respect to time at a given location.

Fig. 1 Schematic representation of flow regimes and boundaries on a stability map



The above flow regimes are presented schematically on a stability map as shown in Fig. 1. The concept of stability map was first used by Poloski et al. (2009a, b) to represent deposition velocity as a function of fluid rheology. The stability map is developed by plotting the viscosity function on the *x*-axis and the slurry flow velocity on the *y*-axis. The boundaries between the flow regimes include (1) the critical deposition boundary, (2) the transitional deposition boundary and (3) the laminar deposition boundary (Poloski et al. 2009a, b; Yokuda et al. 2009). These boundaries demarcate different solid transport mechanisms and are strongly dependent on slurry rheology (Poloski et al. 2009a).

The generalized two-parameter rheology model

Slurries exhibit complex rheology. This is because slurry systems are characterized by complex particle shapes, particle size distributions and inter-particle forces which result in non-Newtonian behavior. A fluid (or slurry for this matter) whose viscosity varies with applied shear rate is generally termed as a Non-Newtonian fluid (Poloski et al. 2009a; Rensing et al. 2008; Ma and Zhang 2008). Dealing with slurries therefore requires a more robust rheological model.

To accommodate the different rheology behaviors, the pipe wall shear stress can be defined in terms of the generalized two-parameter rheological model (Ozbayoglu 2002) as follows in Eq. (1)

$$\tau = \mathbb{K} \left(\frac{8V}{D} \right)^N, \tag{1}$$

the Reynolds number as follows in Eq. (2)

$$Re_G = \frac{8^{1-N} \rho V^{2-N} D^N}{\mathbb{K}}, \tag{2}$$

the Reynolds number as follows in Eq. (2), where *N* and \mathbb{K} are the generalized rheological parameters and can be established in terms of the common rheological parameters as shown in Eqs. (3) and (4)

$$N = \begin{cases} 1 & \text{for Newtonian} \\ n & \text{for power law} \\ \frac{1 - \frac{4}{3} \frac{\tau_Y}{\tau_w} + \frac{1}{3} \left(\frac{\tau_Y}{\tau_w} \right)^4}{1 - \left(\frac{\tau_Y}{\tau_w} \right)^4} & \text{for Bingham Plastic,} \end{cases} \tag{3}$$

$$\mathbb{K} = \begin{cases} \mu & \text{for Newtonian} \\ K \left(\frac{3n+1}{4n} \right)^n & \text{for power law} \\ \tau_w \left(\frac{3\mu_B \tau_w^3}{3\tau_w^4 + \tau_Y^4 - 4\tau_Y \tau_w^3} \right)^N & \text{for Bingham Plastic} \end{cases} \tag{4}$$

The pipe wall shear stress can be easily calculated from the pressure drop per unit length, given as the following equation:

$$\tau = \frac{D}{4} \left(\frac{dp}{dl} \right), \tag{5}$$

The generalized two-parameter model is then used to extend deposition velocity models to non-Newtonian fluids.

Deposition boundary and governing equations

Critical deposition boundary

As the viscosity increases, drag on the particles increases, thus reducing the flow velocity needed to suspend the particles in turbulent flow. To model this boundary, Oroskar and Turian (1980) and Shook et al. (2002) have

been recommended as potential candidates (Poloski et al. 2009a, b). The Oroskar and Turian (1980) model is limited to Newtonian rheology, and therefore, adjustments must be made to extend its applicability to non-Newtonian rheology. The critical deposition velocity model developed by Oroskar and Turian (1980) is presented in Eq. 6.

$$V_c = \sqrt{gd(S-1)} * 1.85C_s^{0.154}(1 - C_s)^{0.356} * \left[\frac{D}{d}\right]^{0.378} * \left[\frac{\rho_f D \sqrt{gd(S-1)}}{\mu_m}\right]^{0.09} \chi^{0.3} \tag{6}$$

where χ is the hindered settling factor and S is the ratio of the solid density to carrier fluid density, ρ_s/ρ_f .

A hindered settling factor of 0.95 has been found to satisfactory for high-volume solid fraction slurries (Poloski et al. 2009a).

By setting $g = 9.8 \text{ ms}^{-2}$ and $\chi = 0.95$, then re-arranging yields

$$V_c = 6.32D^{0.468} d^{0.168} C_s^{0.154} (1 - C_s)^{0.356} (S - 1)^{0.545} \left[\frac{\rho_f}{\mu_m}\right]^{0.09} \tag{7}$$

Because of the particle size limitation in the Oroskar and Turian (1980) model, Thomas’ model should be used for solid particles less than 100 microns (Poloski et al. 2009a, b).

Thomas (1979) equation is written as

$$V_c = 9 \left[\frac{g\mu_w}{\rho_f} (S - 1)\right]^{0.37} \left[\frac{D\rho_f}{\mu_w}\right]^{0.11} \tag{8}$$

This equation can be re-arranged as follows;

$$V_c = 21D^{0.11} (S - 1)^{0.37} \left[\frac{\mu_w}{\rho_f}\right]^{0.26} \tag{9}$$

Therefore, the critical deposition boundary for Newtonian slurries can be represented as follows

$$V_c = \begin{cases} 21D^{0.11} (S - 1)^{0.37} \left[\frac{\mu_w}{\rho_f}\right]^{0.26} & \text{for } d \leq 100 \mu\text{m} \\ 6.32D^{0.468} d^{0.168} C_s^{0.154} (1 - C_s)^{0.356} (S - 1)^{0.545} \left[\frac{\rho_f}{\mu_m}\right]^{0.09} & \text{for } d > 100 \mu\text{m} \end{cases} \tag{10}$$

The slurry viscosity may be determined experimentally or can be approximated by Thomas’ correlation as follows

$$\mu_m = \mu_w (1 + 2.5C_s + 10C_s^2 + 0.0019 \exp^{20C_s}) \tag{11}$$

Extension to non-Newtonian slurries

The critical deposition boundary for non-Newtonian systems can be obtained by replacing the viscosity term in the Oroskar and Turian (1980) model with a generalized viscosity term. Consider a generalized two-parameter viscosity model of the following form.

$$\eta_m = \mathbb{K} \left[\frac{8V}{D}\right]^{N-1} \tag{12}$$

Substituting viscosity term in Eq. 10 with the generalized two-parameter viscosity term in Eq. (12) yields

$$V_c = \left[6.32D^{0.468} d^{0.168} C_s^{0.154} (1 - C_s)^{0.356} (S - 1)^{0.545} \times \left[\frac{8\rho_f}{D\mathbb{K}} \left(\frac{D}{8}\right)^N\right]^{0.09}\right]^{\frac{1}{0.91+0.09N}} \tag{13}$$

Equation 13 is the generalized critical deposition velocity model that predicts the transition from unstable flow to stable turbulent flow.

Transitional deposition boundary

This boundary falls in the high rheology region with increasing non-Newtonian behavior (Poloski et al. 2009a; Peysson 2004; Wilson and Horsley 2004). At point 2, viscous forces dominate the flow and suppress turbulent eddies. Since turbulent eddies are responsible for particle transport, particles will form a bed if the flow transitions from turbulent to laminar (Poloski et al. 2009a, b; Yokuda et al. 2009). This means that particles will settle unless the velocity is increased and the flow becomes turbulent (Poloski et al. 2009a). Also, a higher velocity is necessary to suspend the particles as the viscosity increases. This boundary can be modeled using laminar to turbulent transition model.

The transition from laminar occurs at the critical generalized Reynolds number of $Re_{G,t}$ defined in Eq. 14 (Dodge and Metzner 1959)

$$Re_{G,t} = 3250 - 1150N \tag{14}$$

The transition velocity from laminar, V_t , can then be established by equating critical generalized Reynolds number (Eq. 14) to the generalized Reynolds number (Eq. 2) and re-arranging as shown in Eq. 15.

$$V_t = \left[\frac{3250 - 1150N}{D\rho_f} * \mathbb{K} \right]^{\frac{1}{2-N}} \left[\frac{8}{D} \right]^{\frac{N-1}{2-N}} \quad (15)$$

Equation 15 is the generalized transitional deposition velocity model that predicts the transition from laminar flow to stable turbulent flow.

Laminar deposition boundary

At point 3, the gel strength and/or yield stress forces are large enough to suspend the particles in the stagnant core region (Poloski et al. 2009a). The boundary can be modeled using the Gillies et al. (2007) criterion. Gillies et al. (2007) proposed a criterion based on the ratio, α , of the wall shear stress, τ_w , to the surficial particle shear stress (also known as the gel strength), τ_p (Gillies et al. 2007). The surficial particle shear stress equation developed by Wilson and Horsley (2004) is shown in Eq. 16.

$$\tau_p = \frac{(\rho_s - \rho_f)gd}{6} \quad (16)$$

and the ratio, α , is defined as follows

$$\alpha = \frac{\tau_w}{\tau_p} \quad (17)$$

Settling is nearly eliminated when $\alpha \geq 100$ (Poloski et al. 2009a; Gillies et al. 2007). By choosing $\alpha = 100$ and $g = 9.8 \text{ ms}^{-2}$ and combining Eqs. 16 and 17, it yields

$$\tau_w = 163(S - 1)\rho_f d \quad (18)$$

The laminar transition velocity can be obtained by combining Eqs. 1 and 18, which yields

$$V_l = \frac{D}{8} \left[\frac{163(S - 1)\rho_f d}{\mathbb{K}} \right]^{\frac{1}{N}} \quad (19)$$

Equation 19 is the generalized laminar deposition velocity model that predicts stable laminar flow.

In summary, a new slurry flow regime classification is discussed and models representing flow regime boundaries developed. The new proposed flow regime classification and the models describing their boundaries are summarized in Fig. 2. The generalized parameter \mathbb{K} is used on the x -axis to represent the viscosity function.

For the given set of solid properties, test conditions and fluid properties, the model can be used to generate flow regime boundaries. This may be used as guide in selecting carrier fluid properties and pipe size for the given solids to be transported.

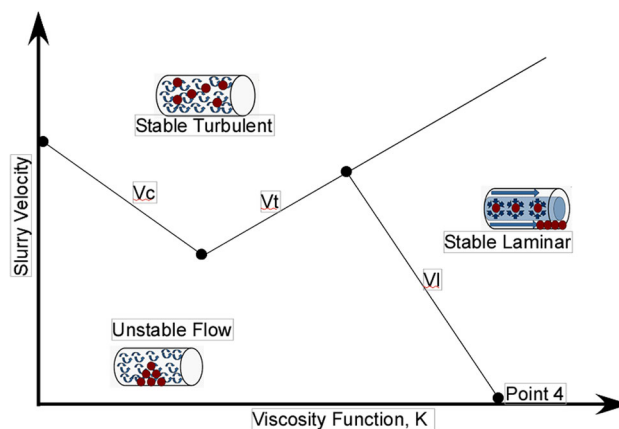


Fig. 2 Proposed slurry flow map with the models describing the boundaries

Table 1 Input parameters used for the base case

Inputs	
Watercut	50 (%)
Pipe diameter	0.078 (m)
Particle diameter	1000 (micron)
Oil density	850 (kg m ⁻³)
Solid density	950 (kg m ⁻³)
Critical Reynolds number	2100 (-)
N	0.9 (-)
\mathbb{K}	0.5 (Pa s ^N)
Solid fraction	0.2 (-)
Carrier fluid density	930 (kg m ⁻³)

Sensitivity analysis on the model performance

Sensitivity analysis was performed on the slurry stability map model by varying input parameters in order to observe their influence on deposition velocity boundaries. The base case input values used in the analysis are summarized in Table 1. The parameters varied were the generalized rheological parameter N , density of the solid particles, carrier fluid density, the critical Reynolds number, pipe diameter and particle diameter.

Effect of the slurry generalized flow behavior index, N

Simulations were done for generalized flow behavior indices of 0.9 and 1.0. The laminar region decreased with increasing shear thinning effects. The transition velocity to turbulent decreased with increasing shear thinning effects, whereas the transition velocity to laminar increased with increasing shear thinning effects as shown in Fig. 3. Therefore, the laminar regime shrinks with

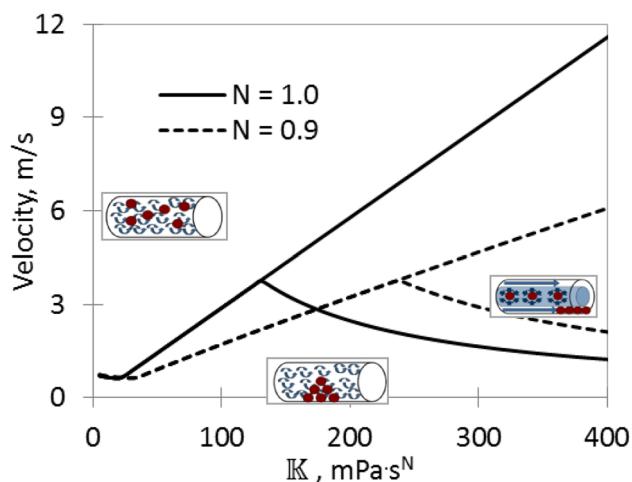


Fig. 3 Model sensitivity on the generalized flow behavior index

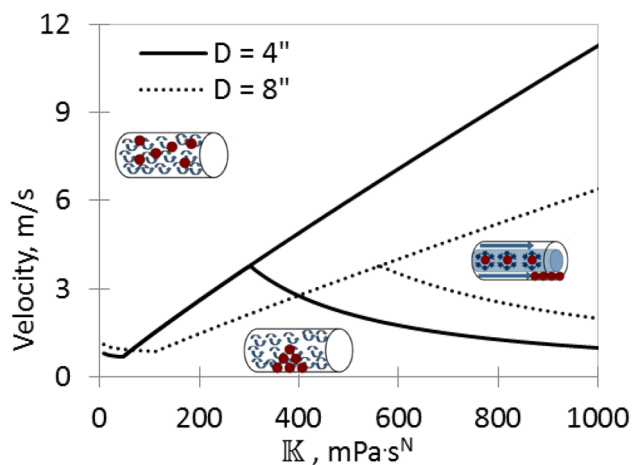


Fig. 4 Sensitivity on the pipe diameters

increasing shear thinning behavior. This means that it is easier to transport solids with Newtonian fluids under laminar flow. On the other hand, it is easier to transport solids with shear thinning fluids under turbulent flow. In other words, high viscosity fluids should be used when transporting solids with Newtonian fluids but operate at high velocities if using shear thinning fluids.

Effect of the pipe diameter, D

Simulations were done for pipe diameters including 4" and 8". Assuming the same velocity, slurry properties and solid particle properties, the laminar region decreases with increasing pipe diameter as shown in Fig. 4. This means that it is easier to transport solids in small pipe diameters under laminar flow. This is because Reynolds number increases with pipe diameter.

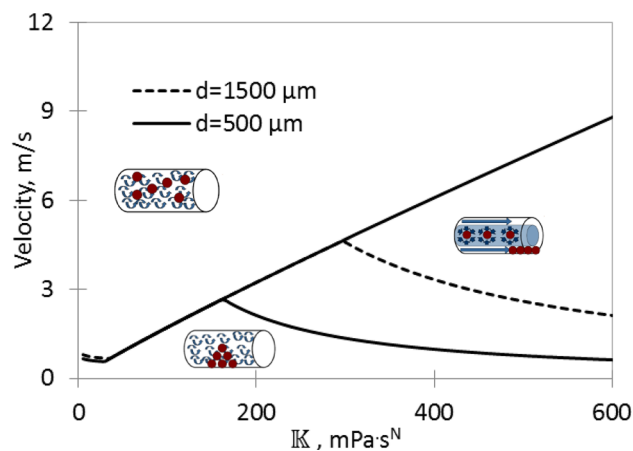


Fig. 5 Sensitivity on the particle diameters

Effect of particle diameter, d

Simulations were done for different particle diameters including 500 microns (1/64") and 1500 microns (4/64"). Assuming the same carrier fluid properties and same testing conditions, the laminar region (particularly the laminar deposition boundary) decreases with increasing particle diameter as shown in Fig. 5. However, the resulting slurry rheology is dependent on particle size, particle distribution and particle morphology, and therefore, effects of particle size on deposition velocity are difficult to isolate.

Effect of solid particle density, ρ_s

Simulations were done for different solid particle densities including 800 kg/m³ (50 lb/ft³) and 1200 kg/m³ (75 lb/ft³). The critical deposition velocity and the laminar deposition velocity increase with increasing particle density, whereas the transitional deposition velocity remains unchanged as shown in Fig. 6. This suggests that transition to turbulent is governed by carrier fluid properties and flow geometry and not the solid particle properties. Lighter particles can easily be suspended into homogeneous suspensions at low shear rate and low carrier fluid viscosity than heavier particles. Similarly, lighter particles can easily be transport under laminar flow by high viscosity carrier fluid than heavier particles.

Model performance on work done by Poloski et al. (2009a, b)

The experimental work done by Poloski et al. (2009a) is relevant for hydrate studies because of the particles size distribution used and the rheology of slurries generated. They used glass beads with diameters ranging from 10 to 300 microns at concentration of 8–12 volume percent generating slurries with Bingham plastic behavior.

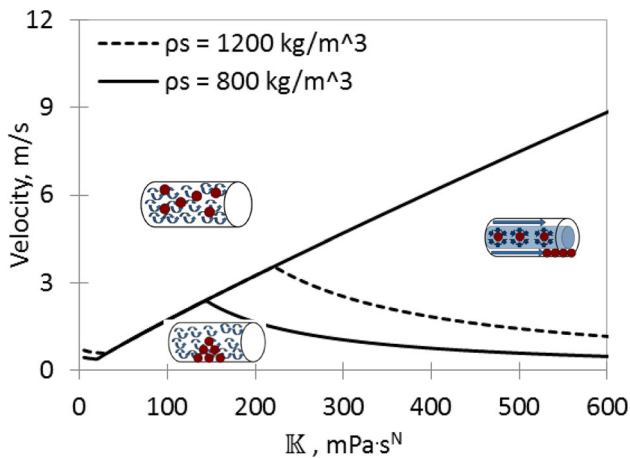


Fig. 6 Sensitivity on the solid particle densities

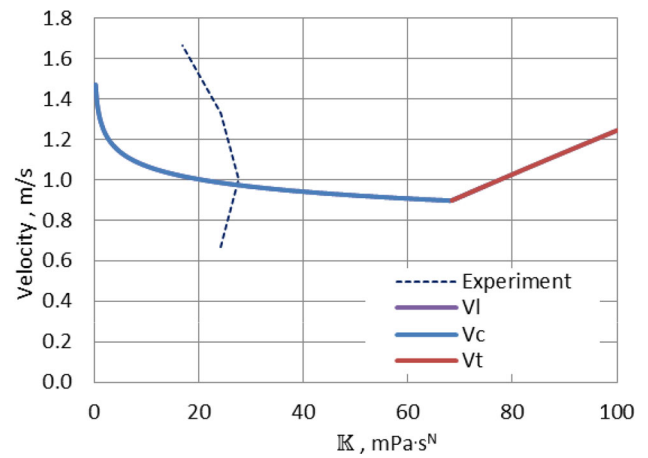


Fig. 7 Stability map for test a

Stainless steel beads were also used to study effects of higher-density particles. The rheology of the slurries was adjusted using clay. They used a flowloop of 5.7 m length and 0.076 m diameter. The deposition velocity was determined by plotting pressure drop as a function of mixture velocity. The deposition velocity was taken to be the velocity at which minimum pressure drop was observed. Table 2 summarizes the properties of solids and slurries used in determining the deposition velocity.

Data from the above table were used together with the measured pressure drop values to calculate the generalized rheological parameters N and K using Eqs. 3 and 4, respectively, and to generate stability maps for these tests. Figure 7 shows the stability map for test a. This test was conducted with low yield stress slurry, and the model predicts deposition in the low rheology region as shown by the blue line. The interception of K values calculated from the experimental data and the simulated map is the deposition velocity. For this test, the predicted deposition velocity is 0.97 m/s and the observed deposition velocity is 1.17 m/s. Figure 8 compares the predicted deposition velocity to the observed values.

From Fig. 8, model predictions show good agreement with the experimental observation. Generally, the model

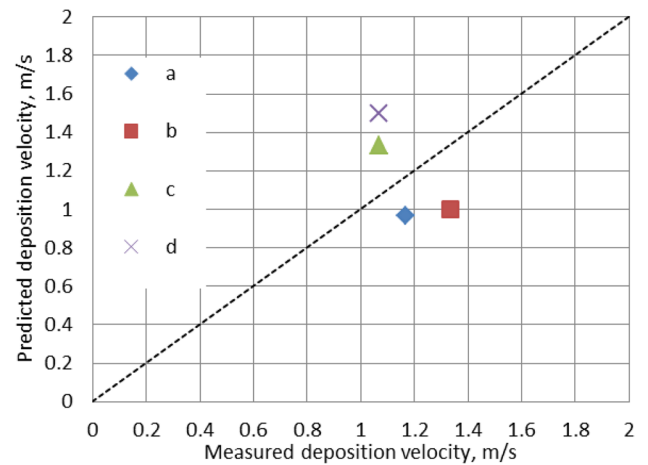


Fig. 8 Comparison between model prediction and experimental data for deposition velocity

overpredicted high-density solids (stainless steel beads) and underpredicted low-density solids (glass beads). Increase in yield stress increased the error on the model prediction.

Table 2 Properties of solids and slurries used in determining the deposition velocity

Exp. no.	Material	Particles diameter (microns)	Solid fraction (vol %)	Solid density (kg m ⁻³)	Slurry rheology (-)	Yield stress (Pa)	Plastic viscosity (mPa s)
a	Glass	141	8.4	2500	Bingham plastic	3.4	5.5
b		200	10.7			6.1	8.7
c	Stainless steel	37	9.5	7950		3.0	7.3
d		28	9.8			6.8	12.4

Conclusions

Theoretical and experimental investigations have been conducted to study particles deposition velocity in complex rheology systems. A summary of observations and conclusions are presented below:

1. The Oroskar and Turian (1980) deposition velocity model for Newtonian system is extended to non-Newtonian systems by replacing the simple Newtonian viscosity term with a more robust two-parameter generalized model. The developed model enables determination of the deposition velocity for any given rheology.
2. A new flow regime classification is proposed and boundaries mathematically modeled. The flow regimes are represented on the stability flow map which demarcates them. On this map, the homogeneous slurries are predicted at low rheology and high mixture velocity, whereas heterogeneous slurries (with a concentration gradient) predicted at high rheology (yield stress effects).
3. Comparison between the model and experimental data with non-interacting particles (glass and stainless steel) reveals good agreement. However, the model overpredicts with the high-density solids (stainless steel beads) and underpredicted with low-density solids (glass beads). Also, increase in yield stress increases the error on the model prediction.

Acknowledgments We would like to thank the member companies of the University of Tulsa Hydrate JIP.

Open Access This article is distributed under the terms of the Creative Commons Attribution 4.0 International License (<http://creativecommons.org/licenses/by/4.0/>), which permits unrestricted use, distribution, and reproduction in any medium, provided you give appropriate credit to the original author(s) and the source, provide a link to the Creative Commons license, and indicate if changes were made.

References

Al-lababidi S, Yan W, Yeung H (2012) Sand transportations and deposition characteristics in multiphase flows in pipelines. *ASME J Energy Resour Technol* 134:034501

Dodge DW, Metzner AB (1959) Turbulent flow of non-Newtonian systems. *AIChE J* 5(2):198–204

Doron P, Barnea D (1996) Flow pattern maps for solid-liquid flow in pipes. *Int J Multiph Flow* 22(2):273–283. doi:10.1016/0301-9322(95)00071-2

Durand R (1953) Basic relationship of the transportation of solids in experimental research. In: Proceedings of the international association for hydraulic research—University of Minnesota, September 1953

Gillies RG, Sun R, Sanders RS, Schaan J (2007) Lowered expectations: the impact of yield stress on sand transport in laminar,

non-Newtonian flows. *J South Afr Inst Min Metall* 107(6):351–357

Ibarra R, Mohan RS, Shoham O (2014) Critical sand deposition velocity in horizontal stratified flow. SPE international symposium and exhibition on formation damage control, Lafayette, Louisiana

King MJS, Fairhurst P, Hill TJ (2001) Solid transport in multiphase flows—application to high-viscosity systems. *ASME J Energy Resour Technol* 123:200–204

Ma ZW, Zhang P (2008) Pressure drop and loss coefficients of a phase change material slurry in pipe fittings. *Int J Refrig* 35:992–1002

McLaury BS, Shirazi SA, Viswanathan V, Mazumder QH, Santos G (2011) Distribution of sand particles in horizontal and vertical annular multiphase flow in pipes and the effects on sand erosion. *ASME J Energy Resour Technol* 133:023001

Najmi K, Hill AL, McLaury BS, Shirazi SA, Cremaschi S (2015) Experimental study of low concentration sand transport in multiphase air-water horizontal pipelines. *ASME J Energy Resour Technol* 137:032908

Newitt DM, Richardson JF, Abbott M, Turtle RB (1955) Hydraulic conveying of solids in horizontal pipes. *Trans Inst Chem Eng* 33:93–113

Oroskar AR, Turian RM (1980) The critical velocity in pipeline flow of slurries. *AIChE J* 26(4):550–558

Ozbayoglu ME (2002) Cuttings transport with foam in horizontal and highly-inclined wellbores. Ph.D. Dissertation, The University of Tulsa, Tulsa, OK

Peysson Y (2004) Solid/liquid dispersions in drilling and production. *IFP J* 59(1):11–21

Poloski AP, Bonebrake ML, Casella AM, Johnson MD, MacFarlan PJ, Toth JJ, Adkins HE, Chun J, Denslow KM, Luna ML, Tingey JM (2009a) Deposition velocities of non-Newtonian slurries in pipelines: complex simulant testing. U.S. Department of energy report prepared by Pacific Northwest national laboratory, PNNL-18316

Poloski AP, Adkins HE, Abrefah J, Casella AM, Hohimer RE, Nigl F, Minette MJ, Toth JJ, Tingey JM, Yokuda ST (2009b) Deposition velocities of Newtonian and non-Newtonian slurries in pipelines. U.S. Department of energy report prepared by Pacific Northwest national laboratory, PNNL-17639

Ramsdell RC, Miedema SA (2013) An overview of flow regimes describing slurry transport. World dredging conference XX, Brussels, Belgium

Rensing PJ, Liberatore MW, Koh CA, Sloan ED (2008) Rheological investigation of hydrate slurries. In: Proceedings of 6th international conference on gas hydrates (ICGH 2008), Vancouver, British Columbia, Canada, July 6–10, 2008

Salama MM (2000) Sand production management. *ASME J Energy Resour Technol* 122:29–33

Shook CA, Gillies RG, Sanders RS (2002) Pipeline hydrotransport with applications in the oil-sand industry. SRC Publication No. 11508-1E02, Saskatchewan Research Council, Saskatoon, Canada

Turian RM, Yuan T (1977) Flow of slurries and pipelines. *Am Inst Chem Eng J* 23(3):232

Turian RM, Hsu FL, Ma TW (1987) Estimation of critical velocity in pipeline flow of slurries. *J Powder Technol* 51:35–47

Wilson KC, Horsley RR (2004) Calculating fall velocities in non-Newtonian (and Newtonian) fluids: a new view. In: Proceedings of 16th international conference hydraulic transport of solids: hydrotransport 16. Santiago, Chile, BHR Group, Cranfield, UK, pp 37–46

Yokuda ST, Poloski AP, Adkins HE, Casella AM, Hohimer RE, Kari NK, Luna ML, Minette MJ, Tingey JM (2009) A qualitative investigation of deposition velocities of non-Newtonian slurry in complex pipelines geometries. U.S. Department of energy report prepared by Pacific Northwest national laboratory, PNNL-17973